Spin caloritronics

Bauer, Gerrit E. W.; Saitoh, Eiji; van Wees, Bart J.

Published in:
Nature Materials

DOI:
10.1038/NMAT3301

Publication date:
2012

nature materials

INSIGHT | REVIEW ARTICLES

PUBLISHED ONLINE: 23 APRIL 2012 | DOI: 10.1038/NMAT3301

Spin caloritronics

Gerrit E. W. Bauer[1,2]*, Eiji Saitoh[1,3] and Bart J. van Wees[4]

Spintronics is about the coupled electron spin and charge transport in condensed-matter structures and devices. The recently invigorated field of spin caloritronics focuses on the interaction of spins with heat currents, motivated by newly discovered physical effects and strategies to improve existing thermoelectric devices. Here we give an overview of our understanding and the experimental state-of-the-art concerning the coupling of spin, charge and heat currents in magnetic thin films and nanostructures. Known phenomena are classified either as independent electron (such as spin-dependent Seebeck) effects in metals that can be understood by a model of two parallel spin-transport channels with different thermoelectric properties, or as collective (such as spin Seebeck) effects, caused by spin waves, that also exist in insulating ferromagnets. The search to find applications — for example heat sensors and waste heat recyclers — is on.

Thermoelectric and thermomagnetic effects have been known for two centuries[1,2]. They reflect the coupling of heat and charge currents and find applications in thermometers, power generators and coolers. Heat currents also interact with spin currents[3–5]. This has spawned the field of spin caloritronics (from 'calor', the Latin word for heat)[6], which is concerned with non-equilibrium phenomena related to spin, charge, entropy and energy transport in (mostly) magnetic structures and devices. Here we will look at theoretical and experimental evidence for spin-dependent Seebeck/Peltier coefficients and thermal conductance, thermal spin-transfer torques, spin and anomalous thermoelectric Hall effects, the recently discovered spin Seebeck effect and so on. We will not discuss equilibrium phenomena such as the temperature dependence of magnetic properties including phase transitions, nor related topics such as magnetocaloric cooling and thermally assisted magnetic recording.

A challenge for condensed-matter and device physics is to develop 'green' information and communication technologies, and efficient devices for scavenging waste heat. Another issue is the imminent breakdown of Moore's law by the thermodynamic bottleneck: further decreases in feature size and transistor speed go in parallel with intolerable levels of ohmic energy dissipation associated with the motion of electrons in conducting circuits. Thermoelectric effects in meso-[7] and nanoscopic[8] structures might help. The additional degree of freedom provided by the electron spin and magnetic order provides new strategies to increase the thermoelectric figure of merit as well as offering radically new functionalities in all temperature regimes. Spin caloritronic effects are not limited to solid-state structures, but have been predicted to occur in cold atomic gases as well[9].

Spin caloritronic phenomena can be roughly classified into (i) independent electron, (ii) collective and (iii) relativistic effects. The first class (i) is the thermoelectric generalization of collinear magnetoelectronics and effects such as giant magnetoresistance and tunnel magnetoresistance. The second class of effects (ii) is generated by the collective dynamics of the magnetic order parameter that couple to single particle spins via the spin-transfer torque and spin pumping. Finally, there are (iii) thermoelectric generalizations of relativistic corrections such as anisotropic magnetoresistance, anomalous Hall effects and spin Hall effects. In what follows, we describe and interpret selected recent experiments to provide a snapshot of a field in motion, rather than a comprehensive review. A brief introduction to the conventional thermoelectrics is given in Box 1. We also make an attempt to harmonize the historically grown and somewhat confusing nomenclature for spin caloritronic effects in Box 2.

Independent electron/spin effects in metallic magnets

Transport in magnetic layered structures with collinear magnetizations is well described by the two-current model, in which the majority and minority spin carriers form parallel channels with different resistances for ferromagnets, as well as interfaces between ferromagnets and paramagnetic metals, and tunnelling barriers between metals if at least one is magnetic. In this section we discuss the basic theoretical concepts of the two-channel resistor model and review recent observations of associated spin caloritronic effects.

Spin-dependent thermoelectrics in metallic magnetic heterostructures. Thermoelectricity in metals is governed by the energy dependence of the electron distribution and conductivity in an energy interval of the order $k_B T$ around the Fermi energy, as sketched in Box 1. Here we generalize the concepts to the two-spin current model. The thermoelectric properties in isotropic and monodomain metallic ferromagnets[3,5,10–12] are affected by the spin-dependent conductivities $\sigma^{(s)}(\varepsilon)$, $s = \uparrow,\downarrow$ being the spin-index, leading to the conventional charge conductance $\sigma = \sigma^{(\uparrow)} + \sigma^{(\downarrow)}$ and Seebeck coefficient $S = (\sigma^{(\uparrow)}S^{(\uparrow)} + \sigma^{(\downarrow)}S^{(\downarrow)})/(\sigma^{(\uparrow)} + \sigma^{(\downarrow)})$. In linear response and using the Sommerfeld expansion $S^{(s)} = -eL_0T\partial \ln \sigma^{(s)}(\varepsilon)/\partial\varepsilon|_{\varepsilon_F}$ (Mott's law[1]), where L_0 is the Lorenz constant, and

$$\begin{pmatrix} \mathbf{J}_c \\ \mathbf{J}_s \\ \mathbf{Q} \end{pmatrix} = \sigma(\varepsilon_F) \begin{pmatrix} 1 & P & ST \\ P & 1 & P'ST \\ ST & P'ST & \kappa T/\sigma \end{pmatrix} \begin{pmatrix} \nabla\mu_c/e \\ \nabla\mu_s/2e \\ -\nabla T/T \end{pmatrix} \quad (1)$$

where $\mathbf{J}_{c(s)} = \mathbf{J}^{(\uparrow)} \pm \mathbf{J}^{(\downarrow)}$ and $\mathbf{Q} = \mathbf{Q}^{(\uparrow)} + \mathbf{Q}^{(\downarrow)}$ are the charge (c), spin (s) and heat currents, respectively, and P and P' stand for the spin-polarization of the conductivity and its energy derivative

$$P = \left.\frac{\sigma^{(\uparrow)} - \sigma^{(\downarrow)}}{\sigma}\right|_{\varepsilon_F}; \; P' = \left.\frac{\partial(P\sigma)}{\partial\varepsilon}\right|_{\varepsilon_F} \quad (2)$$

The expression $\mu_c = (\mu^{(\uparrow)} + \mu^{(\downarrow)})/2$ gives the charge electrochemical potential and $\mu_s = \mu^{(\uparrow)} - \mu^{(\downarrow)}$ the spin accumulation. The spin-dependent thermal conductivities obey the Wiedemann–Franz law $\kappa^{(s)} \approx L_0T\sigma^{(s)}$ when $S^{(\uparrow)/(\downarrow)} << L_0^{1/2}$ and the total thermal conductivity is $\kappa = \kappa^{(\uparrow)} + \kappa^{(\downarrow)} \rightarrow L_0T\sigma$. The symmetry of the spin-dependent thermoelectric matrix in equation (1) reflects Onsager's reciprocity relation[13,14]. We observe a spin current driven by a temperature gradient (the spin-dependent Seebeck effect) as well as a heat current

[1]Institute for Materials Research, Tohoku University, Sendai 980-8577, Japan. [2]Kavli Institute of NanoScience, Delft University of Technology, 2628 CJ Delft, The Netherlands. [3]CREST, Japan Science and Technology Agency, Sanbancho, Tokyo 102-0075, Japan. [4]Zernike Institute for Advanced Materials, University of Groningen, The Netherlands. *e-mail: g.e.w.bauer@imr.tohoku.ac.jp; g.e.w.bauer@tudelft.nl

Box 1 | Thermoelectric essentials.

We learn from textbooks that the electron–hole asymmetry at the Fermi energy in metals generates thermoelectric phenomena as illustrated in Fig. B1. A heat current **Q** then drags charges with it, thereby generating a thermopower electric field **E** or charge current $\mathbf{J}_c$ for open- or closed-circuit conditions, respectively. Vice versa, a charge current is associated with a heat current, which can be used to heat or cool reservoirs or junctions of different materials. In a diffusive bulk metal the relation between the local driving forces, that is, the electric field as voltage gradient $\mathbf{E} = -\nabla_r V$ and the temperature gradient $\nabla_r T$, reads

$$\begin{pmatrix} \mathbf{E} \\ \mathbf{Q} \end{pmatrix} = \begin{pmatrix} 1/\sigma & S \\ \Pi & \kappa \end{pmatrix} \begin{pmatrix} \mathbf{J}_c \\ -\nabla_r T \end{pmatrix} \tag{5}$$

where σ is the electric conductivity, S the Seebeck coefficient (or thermopower) and κ the heat conductivity[1]. The Kelvin–Onsager relation between the Seebeck and Peltier coefficients $\Pi = ST$ is a consequence of the Onsager reciprocity[13]. In the Sommerfeld approximation, valid when the conductivity as a function of energy varies linearly on the scale of the thermal energy $k_B T$ or, more precisely, when $L_0 T^2 |\partial^2_\varepsilon \sigma(\varepsilon)|\varepsilon_F| \ll \sigma(\varepsilon_F)$,

$$S = -eL_0 T \frac{\partial}{\partial \varepsilon} \ln \sigma(\varepsilon)\Big|_{\varepsilon_F} \tag{6}$$

where the Lorenz constant $L_0 = (\pi^2/3)(k_B/e)^2$ and $\sigma(\varepsilon)$ is the energy-dependent conductivity around the Fermi energy ε_F. In this regime the Wiedemann–Franz Law $\kappa = \sigma L_0 T$ holds.

Thermoelectric phenomena at constrictions and interfaces are obtained by replacing the gradients by differences and the conductivities by conductances:

$$\begin{pmatrix} -\Delta V \\ Q \end{pmatrix} = \begin{pmatrix} 1/G & S \\ \Pi & \kappa \end{pmatrix} \begin{pmatrix} J_c \\ -\Delta T \end{pmatrix} \tag{7}$$

Thermoelectric material parameters have been computed from first principles for metallic interfaces[10,11] and tunnelling junctions[29,30] by using the scattering theory of transport[105]. Here a scatterer is considered to be sandwiched between two reservoirs with Fermi–Dirac electronic distribution functions f_L and f_R. The transmission probability as a function of energy is denoted by

$$g(\varepsilon) = \sum_{nm}^{\varepsilon_n = \varepsilon_m = \varepsilon} \left|t_{nm}\right|^2 \tag{8}$$

where t_{mn} is the transmission coefficient of an electron approaching the scatterer at an energy ε in a channel n and leaving it in a channel m on the other side. The charge and heat currents through the junction then read

$$J_c = \frac{e}{h} \int d\varepsilon g(\varepsilon) \left[f_L(\varepsilon) - f_R(\varepsilon) \right] \tag{9}$$

$$Q = \frac{1}{h} \int d\varepsilon g(\varepsilon) \, (\varepsilon - \varepsilon_F) \, [f_L(\varepsilon) - f_R(\varepsilon)] \tag{10}$$

When $g(\varepsilon)$ varies slowly, the integrals can be carried out analytically by the Sommerfeld expansion of the Fermi–Dirac distribution[1], leading to linear expressions for the currents in terms of the electrochemical and temperature bias, equation (7) with:

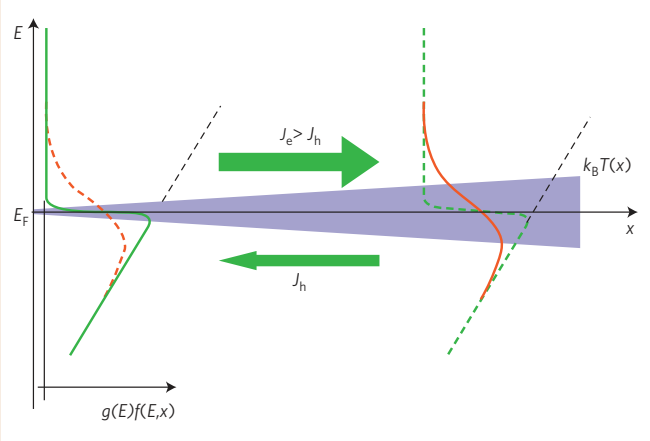

Figure B1 | Heat-current-induced charge current in electric conductors. A temperature difference over the metal in the x direction is represented by thermal broadening of the Fermi–Dirac distribution function. The hot electrons above as well as hot holes below the Fermi energy on the right side diffuse to the left, creating a heat current carried by electrons and holes. In this example the conductance around the Fermi energy increases as a function of energy ('electron-like'), which implies that the electron current is larger than the hole current, causing a net charge current opposite to the heat current. In an open circuit the charge accumulation at the edges gives rise to the thermoelectric voltage.

$$G = \frac{e^2}{h} \sum_{nm}^{\varepsilon_F} \left|t_{nm}\right|^2 \tag{11}$$

$$S = -eL_0 T \frac{\partial}{\partial \varepsilon} \ln g(\varepsilon)\Big|_{\varepsilon_F} \tag{12}$$

A general and intuitive framework to understand transport in (magneto-)electronic devices is circuit theory[79]. It is most effective when a structure or device, such as a metallic multilayer or large quantum dot, is not fully phase coherent, yet quantum effects are important in sections of the sample, such as interfaces or point contacts. The 'nodes' are then the regions in between these 'resistors' and can be described by semiclassical methods. The semiclassical distribution functions in the nodes are governed by local temperatures and chemical potentials. They are connected by scattering matrices that can be computed fully quantum mechanically, for example from first principles. The transmission and reflection probabilities of the resistors are the necessary boundary conditions for the Boltzmann/diffusion equation in the nodes. This approach can be extended to the d.c. and a.c. transport properties of non-collinear magnetic systems[79] including thermoelectric properties[11]. With additional approximations, such as a spatially constant distribution function, the conservation of charge, spin and energy leads to extended Kirchhoff's laws, and analytical results can be obtained to model transport properties of non-trivial circuits and devices.

The efficiency of a thermoelectric device is usually parameterized in terms of a figure of merit Z, where $ZT = S^2\sigma/\kappa_{tot}$ and where κ_{tot} also includes the phonon contribution to the heat conductivity. Although $Z \to \infty$ corresponds to the ideal Carnot efficiency, values of ZT significantly and reproducibly higher than unity have been reported only rarely.

Box 2 | What's in a name?

The independent-electron effects in metallic magnetic structures discussed in the main text are explained in terms of a generalization of classical thermoelectrics to allow for spin-dependent spectral conductivities and, therefore, spin-dependent Seebeck and Peltier coefficients. Their observation in lateral structures by Slachter *et al.*[22] and Flipse *et al.*[23] is therefore appropriately referred to as spin-dependent Seebeck and spin-dependent Peltier effects. By analogy with (giant) magnetoresistance, the dependence of the thermoelectric effects on the magnetic configurations should be referred to as the (giant) magneto-Seebeck effect or magnetothermopower, and the (giant) magneto-Peltier effect. The dependence of the heat resistance on the magnetic orientations is then obviously a (giant) magneto-heat resistance. Following conventions for magnetic tunnel junctions, the 'giant' in the previous expressions should be replaced by 'tunnel' and recent experiments[6,28,31] could be referred to as the 'tunnel magneto-Seebeck effect'. The term 'Seebeck spin tunnelling' chosen in ref. 34 for the thermal spin injection via a tunnelling barrier should not lead to confusion.

The 'spin Seebeck effect' was given its name when not yet fully understood[64]. As explained in the section on collective effects, the physical mechanism is very different from conventional thermoelectrics. The name caught on, however, and at this time it seems wiser not to change it to 'spin wave' or 'magnonic' Seebeck effect, but pragmatically stick to the original one. This should not cause confusion as long as we adhere to the 'spin-dependent' label for the single-electron effects as proposed above.

driven by spin accumulation (directly related to the spin-dependent Peltier effect), both proportional to $P'ST$.

In equation (1), the spin heat current $\mathbf{Q}_s = \mathbf{Q}^{(\uparrow)} - \mathbf{Q}^{(\downarrow)}$ does not appear. This is a consequence of the implicit assumption that a spin temperature (gradient) $T_s = T^{(\uparrow)} - T^{(\downarrow)}$ is effectively quenched by interspin and electron–phonon scattering[10]. This approximation does not necessarily hold at the nanoscale and at low temperatures[15,16]. The presence of spin temperatures can be observed, for example, as a violation of the Wiedemann–Franz Law or a magneto-heat conductance in spin valves[10].

According to equation (1), not only an applied voltage but also a temperature gradient drives a spin current in a conducting ferromagnet. Conservation of charge and spin currents at a contact between the ferromagnet (FM) and a normal metal (NM) then implies spin current injection into NM under a voltage as well as a temperature bias[3,5,12]. A thermally or electrically created spin accumulation can be detected by a switchable second ferromagnet, either electrically by the induced voltage or through temperature changes due to the Peltier effect. In magnetic clusters embedded in a normal metal matrix, the thermally injected spin accumulation contributes to the magnetothermopower[17,18].

Spin-dependent Seebeck and Peltier effects. The thermoelectric generalization of the (giant) magnetoresistance in FM|NM|FM metallic spin valves — that is, the difference between the properties for parallel and antiparallel magnetic configurations — is referred to as the (giant) magneto-Peltier and magneto-Seebeck effect/magnetothermopower[10,12,19]. The magneto-Seebeck effect has been observed in multilayered magnetic nanowires[5]. A large Peltier effect in constantan (CuNi alloy)/Au nanopillars[19] has been associated with phase separation[21].

A spin-dependent Seebeck effect has been demonstrated in lateral spin-valve structures[22]. Here a temperature gradient is generated over an interface by resistive heating of a ferromagnet (FM_1 in Fig. 1a). Figure 1b shows the spin-dependent chemical potentials $\mu^{(\uparrow)}$,$\mu^{(\downarrow)}$ across the FM_1|NM interface when a heat current Q crosses it but charge current is zero. Because the heat current is conserved, ∇T is discontinuous at the interface. The slopes of the electrochemical potentials in FM and NM reflect the charge Seebeck coefficients of the bulk materials. Because the individual Seebeck coefficients for the two spin channels $S^{(\uparrow)}$ and $S^{(\downarrow)}$ are not equal, a spin current proportional to $S^{(\uparrow)} - S^{(\downarrow)}$ flows through FM even in the absence of a charge current, creating a spin accumulation $\mu^{(\uparrow)} - \mu^{(\downarrow)}$ close to the interface, which relaxes in the FM and NM on the length scale of their respective spin-flip diffusion lengths λ_F and λ_N. A thermoelectric interface potential $\Delta\mu = P\mu_s$ also builds up. On the left side no spin current is allowed to leave, and the spin-dependent Seebeck effect results in a spin accumulation of opposite sign. Owing to the spin-dependence of the Seebeck coefficient, the heat current Q thereby induces a spin current into the normal metal. Slachter *et al.*[22] detected the spins thus accumulated by means of the voltage difference V with respect to an analysing ferromagnetic contact FM_2. Because FM_1 and FM_2 have different coercive fields, the spin accumulation is revealed by the voltage traces $V(H)$ as a function of magnetic field H.

A spin-dependent Peltier effect has been discovered recently in a dedicated lateral/perpendicular nanostructure (Fig. 2). The

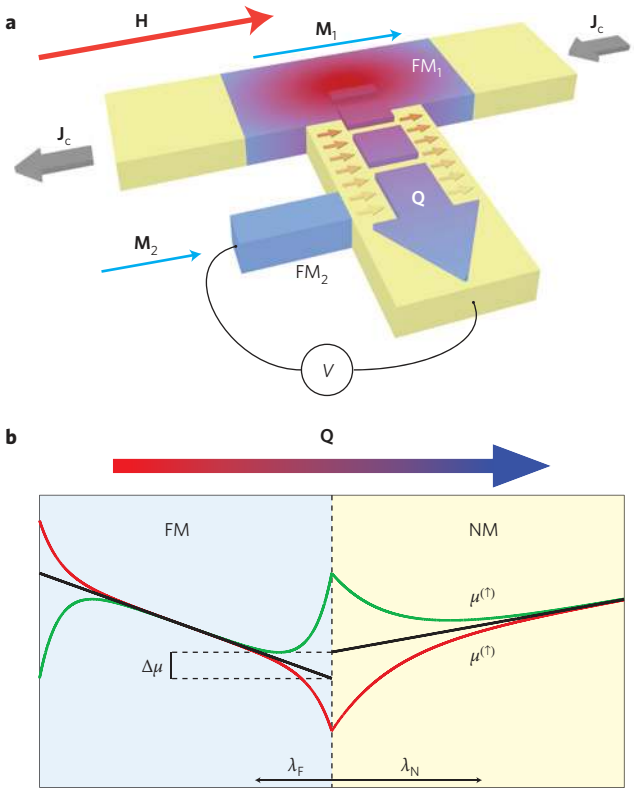

Figure 1 | Non-local detection of thermally injected spin accumulation (spin-dependent Seebeck effect). a, Sketch of the measuring device. **b**, Schematics of thermal spin injection by the spin-dependent Seebeck effect across an FM|NM interface (symbols are explained in the text). For the purpose of illustration, the charge Seebeck coefficients have been chosen to be small in order not to mask the spin accumulation generated by the spin-dependent Seebeck effect. Figure reprinted from ref. 22, © 2010 NPG.

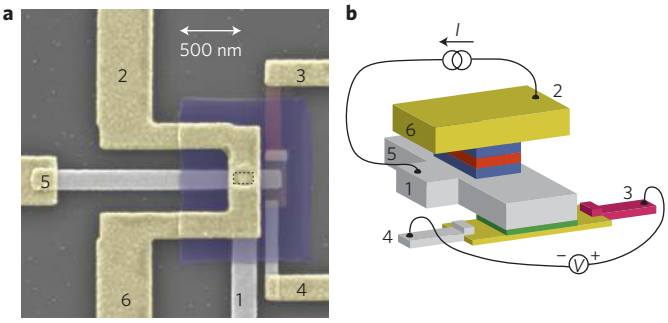

Figure 2 | Device geometry of the spin-dependent Peltier effect. a, Scanning electron microscopy image of the measuring device. The colours represent the different materials used. Yellow: gold top contact; grey: platinum bottom contacts; blue: cross-linked PMMA; red: constantan ($Ni_{45}Cu_{55}$). **b**, Schematic representation of the device. Current is sent from contact 1 to 2 while the voltage is recorded between contacts 3 and 4. Contacts 1, 2, 5 and 6 are used for four-probe spin-valve measurements. The thermocouple is electrically isolated from the bottom contact by an Al_2O_3 (green) layer. The perpendicular giant magnetoresistance stack for the spin-accumulation injection consists of 15 nm $Ni_{80}Fe_{20}$ (permalloy)|15 nm Cu|15 nm $Ni_{80}Fe_{20}$ (ref. 23). The observed spin-dependent Peltier coefficients are consistent with the results from ref. 22 and the spin-dependent Kelvin–Onsager relation $\Pi^{(s)} = S^{(s)}T$. Figure reprinted from ref. 23, © 2012 NPG.

heat current induced by injecting a spin accumulation into the ferromagnet was detected in terms of the associated temperature changes by a thermocouple[23,24].

Tunnel junctions. The electrical resistance of FM|I|FM magnetic tunnel junctions, where I denotes an electric insulator, depends on the magnetic configuration, leading to huge tunnel magnetoresistance ratios. Large tunnelling magneto-Seebeck, magneto-Peltier and magneto-heat resistance effects may be expected[25,26]. A magneto-Seebeck effect in MgO-based magnetic tunnel junctions has been observed under heat gradients created electrically[27] and optically[28]. Results can be compared with *ab initio* calculations[29,30]. Large Seebeck and magneto-Seebeck effects were found for magnetic tunnel junctions with amorphous Al_2O_3 barriers that were interpreted in terms of the Jullière model[31]. A spin-dependent thermopower has been predicted from first principles for molecular spin valves[32].

As discussed by Jansen *et al.*[33] in this issue, the spins injected into semiconductors can be detected in a three-terminal structure with only one magnetic contact, which acts as an injector as well as a detector of spins. The spin-related signal can be disentangled by the Hanle effect — that is, the dephasing of the spin accumulation by a transverse magnetic field. Le Breton *et al.*[34] showed that (Joule) heating of a ferromagnet contact to Si with alumina barriers leads to Hanle curves that prove the presence of a thermally injected spin accumulation. This effect was measured at room temperature and referred to as Seebeck spin tunnelling.

A low-temperature tunnelling anisotropic magnetothermopower has been observed in (Ga,Mn)As|i-GaAs|n-GaAs structures[35]. Here the spin dependence is evident by the uniaxial symmetry of the thermovoltage as a function of the magnetization direction, reflecting the strong spin–orbit interaction in the GaAs valence band.

Collective effects

Ferromagnetism is a quantum coherent ground state with broken rotational and time-reversal symmetry. Its extraordinary robustness is reflected in critical temperatures up to 1,400 K. Magnetization is also resilient against spatial deformations. In nanoscale structures, the magnetization dynamics are often well described by a single time-dependent vector, the 'macrospin' model. In extended systems the elementary excitations are spin waves or magnons[36,37]. The magnetization interacts with the electron charge current through spin-transfer torques and spin pumping, as discussed by Brataas *et al.*[38] in this issue. Here we focus on phenomena such as heat-current-induced magnetization dynamics, as well as the related 'spin Seebeck effect'.

The heat current that travels by means of spin waves (magnons) carries spin angular momentum opposite to that of the magnetization[39,40], as sketched in Fig. 3b. In metallic ferromagnets, the magnon spin current runs in parallel with the conventional particle current. The two modes interact weakly, causing, for example, a current-induced Doppler shift of spin waves[41], contributions to the spin-dependent Seebeck coefficients[42], and the dissipative part of the current-induced spin-transfer torque[43]. The magnon-drag effect on the thermopower of permalloy has been observed recently in nanostructured lateral thermopiles[44]. Spin waves can be actuated and detected electrically even in magnetic insulators[45].

At elevated temperatures, phonons, electron–hole excitations and magnons coexist and carry heat currents in parallel. Most non-equilibrium states are well explained in terms of a weakly interacting three-reservoir model, in which phonons, electrons and magnons are at separate thermal equilibria with possibly different temperatures[46]. The coupling of different modes can be important for thermoelectric phenomena such as the phonon-drag effect on the thermopower at low temperatures.

Thermal spin-transfer torques. In the presence of a non-collinear magnetic texture, either in a heterostructure such as a spin-valve and tunnel junction, or a magnetization texture such as a domain wall or magnetic vortex, the magnetic order parameter absorbs a spin current or rotates its polarization. According to the conservation law of angular momentum, this is equivalent to a torque on the magnetization that, if strong enough, leads to coherent magnetization precession and ultimately magnetization reversal[47]. A heat current can exert a torque on the magnetization as well[10], leading to thermally induced magnetization dynamics[48]. Such a torque acts under closed-circuit conditions, in which part of the torque is exerted by charge currents induced by the conventional thermopower, as well as in an open circuit without charge currents[10].

The angular dependence of the thermal torque can be computed by circuit theory[10,12] (Box 1). Indications for a thermal spin-transfer torque have been found in experiments on nanowire spin valves[49]. Slonczewski[50] studied the spin-transfer torque in spin valves in which the polarizer is a magnetic insulator that exerts a torque on a free magnetic layer in the presence of a temperature gradient. The thermal torque is found to be far more efficient at switching magnetizations than a charge-current-induced torque, but the parasitic heat conductance channels may spoil the advantage. Note that the physics of heat-current-induced spin injection by magnetic insulators is identical to that of the longitudinal spin Seebeck effect, as discussed below.

Thermal torques have been predicted by first-principles calculations for magnetic tunnel junctions with thin barriers[30]. At ambient conditions the critical temperature difference over the barrier for switching from antiparallel to parallel configurations is estimated to be 6 K, but it must be an order of magnitude larger to switch back. The large torques for the antiparallel configuration can be explained by interface states in the thermal window close to the Fermi energy on one side of the barrier, which allow for multiple scattering processes that lead to very efficient spin transfer close to antiparallel configurations.

Domain-wall motion induced by charge currents[47] can be understood in terms of angular momentum conservation in the adiabatic

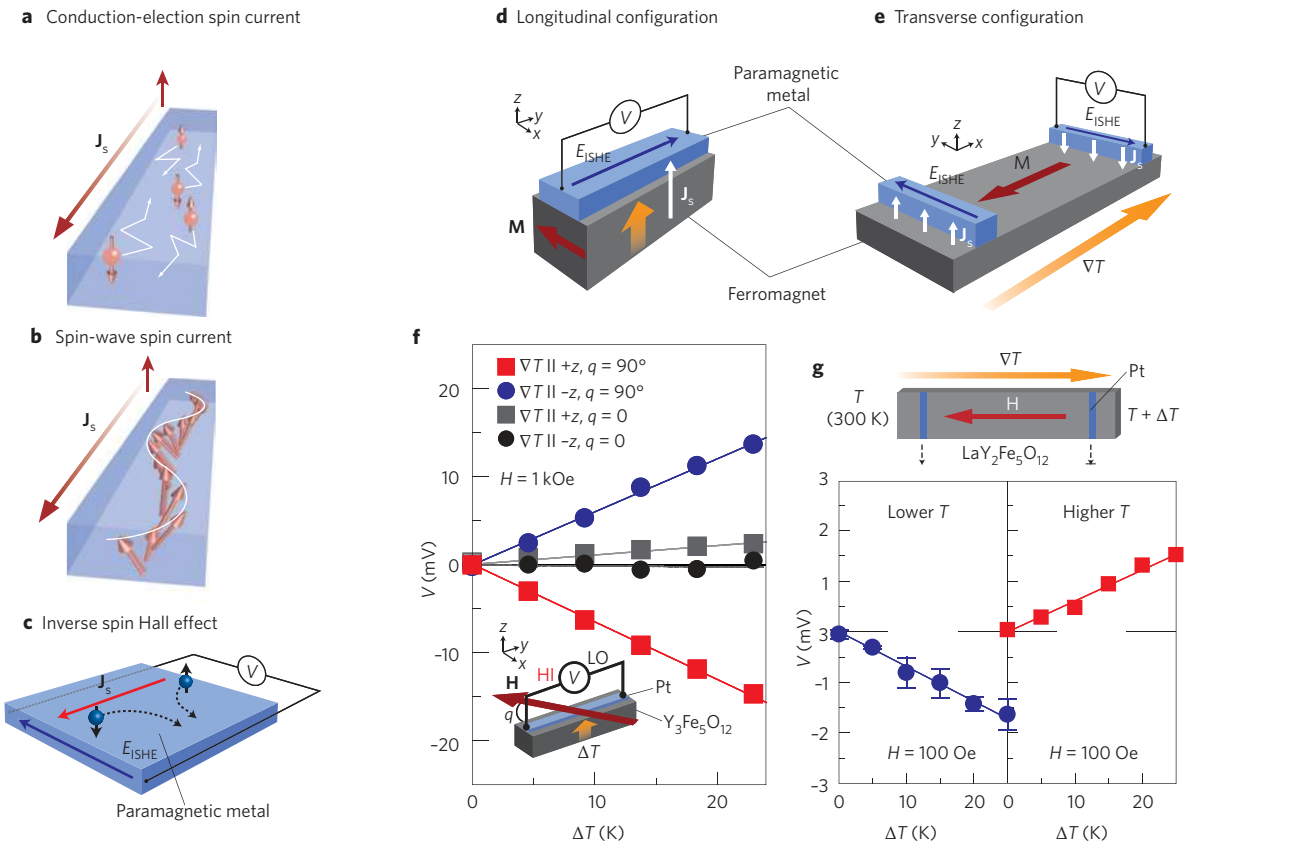

Figure 3 | Collective spin dynamics and spin Seebeck effect in magnetic insulators. Spin currents can be carried by **a**, free electrons and **b**, spin waves (adapted from ref. 45, © 2010 NPG). **c**, Spin currents injected into a paramagnetic metal ($\mathbf{J}_s$) can be detected by the inverse spin Hall effect in terms of the electromotive force E_{ISHE} generated by the spin–orbit interaction. The observable is the voltage V that builds up normal to the spin current. **d**,**e**, The spin Seebeck effect can be observed in two different configurations, the longitudinal and the transverse, as illustrated schematically in **d** and **e** respectively. **f**,**g**, Experimental data are shown for the longitudinal (**f**)[86] and transverse (**g**) spin Seebeck effect in yttrium iron garnets [69,85].

regime, in which the length scale of magnetization texture such as the domain-wall width is much larger than the scattering mean free path or Fermi wavelength, as appropriate for most transition metal ferromagnets. In spite of initial controversies, the importance of dissipation in the adiabatic regime[51] is now generally appreciated. In analogy to the Gilbert damping factor α, the dissipation under an applied current is governed by a material parameter β_c that for itinerant magnetic materials is of the same order as α (ref. 51; for a review see ref. 52). In the presence of electron–hole asymmetry at the Fermi energy, the adiabatic thermal spin transfer torque[10] is associated with a dissipative β_T correction[53,54], which has been explicitly calculated for GaMnAs (ref. 55). Non-adiabatic corrections to the thermal spin-transfer torque in fast-pitch ballistic domain walls have been calculated by first-principles[56]. Laser-induced domain-wall pinning might give clues for heat current effects on domain-wall motion[57].

Spin waves can move domain walls, leading to domain-wall motion in the opposite direction to the spin-wave propagation[58,59]. Recently, this topic has been addressed in the modern context of heat-current-induced domain-wall motion in magnetic insulators that induces motion to the hotter edge of the wire[60–63].

Spin Seebeck effect. The spin Seebeck effect is the transverse electromotive force in a paramagnetic contact to a ferromagnet by a temperature bias, as illustrated in Fig. 3d and e for the two principal sample geometries. This effect is interpreted in terms of a spin current injected into the normal metal by the ferromagnet[64] that is transformed into an electric voltage by the inverse spin Hall effect (ISHE)[65–67] (Fig. 3c). The ISHE is caused by the bending of electron orbits of up and down spins into opposite directions normal to their group velocity, owing to the spin–orbit interaction. It generates a relatively large voltage for heavy metals such as Pt while being virtually absent for Cu, and it has the advantage of scaling linearly with the wire length (for details see Jungwirth *et al.* in this issue[68]).

The spin Seebeck effect was discovered first in permalloy[64], and later in electrically insulating yttrium iron garnet (YIG)[69], ferromagnetic semiconductors (GaMnAs)[70] and Heusler alloys[71], with very similar phenomenology. Its physics is completely different from the spin-dependent Seebeck effect discussed above, because the conduction electron contribution is negligible[72] (see, however, ref. 73). This became obvious only after the observation of the spin Seebeck effect generated by an insulating ferromagnet[69] (Fig. 3f,g). The spin current is the result of a thermal non-equilibrium at the interface between the ferromagnet and the normal conductor, as explained in the following in terms of an imbalance of the thermally excited spin currents over the interface by spin pumping[74] and spin torques[47].

Consider first a ferromagnet at thermal equilibrium with an attached normal metal contact (Fig. 4a). When the ferromagnet is thermally excited, by its time dependence the magnetization $\mathbf{m}(t)$ 'pumps' a net spin current into the normal metal[74]

$$\mathbf{J}_s^{\mathrm{pump}}(t) = \frac{\hbar g_r}{4\pi}\,\mathbf{m}(t) \times \frac{\mathrm{d}\mathbf{m}(t)}{\mathrm{d}t} \qquad (3)$$

where g_r is the real part of the (dimensionless) spin-mixing conductance of the FM|NM interface. On the other hand,

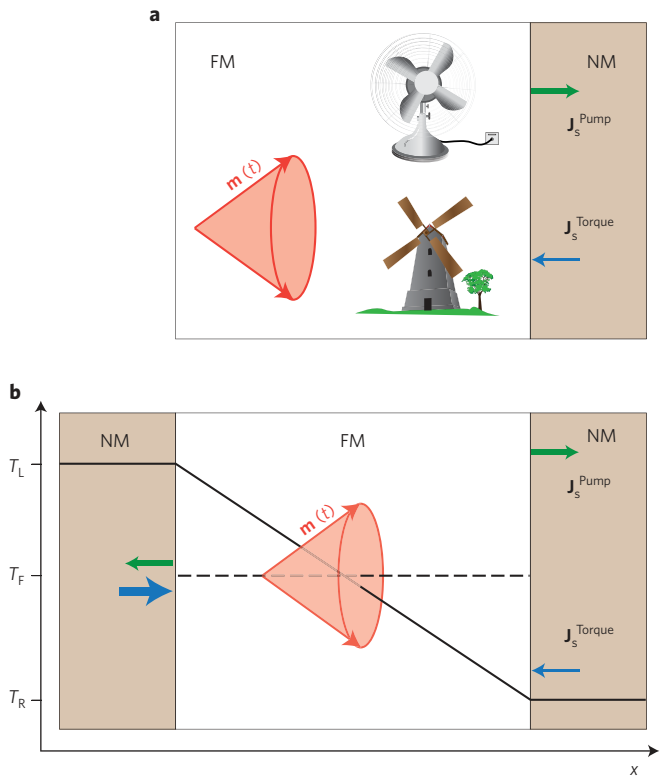

Figure 4 | Thermal fluctuations and spin currents. a, A bilayer of a ferromagnet (FM) and a paramagnetic metal (NM). **b**, An NM|FM|NM sandwich with temperature bias $T_R - T_L$, where T_R and T_L are the temperatures of the left and right reservoirs, and T_F the temperature of the magnetic order. The fluctuations in the magnetization direction vector $\mathbf{m}(t)$ pump spin currents J_s^{pump} and J_s^{torque}. They are cancelled on average by fluctuating Johnson–Nyquist spin currents at thermal equilibrium[75], but in the presence of a temperature bias, net spin (and heat) currents flow with magnitudes indicated by the thickness of the arrows.

at finite temperatures the normal metal generates thermal (Johnson–Nyquist) noise in the form of current fluctuations that are partially spin-polarized[75]. These lead to random spin-transfer torques that, vice versa, generate magnetization dynamics. At thermal equilibrium the sum of the time-averaged currents vanishes, by the second law of thermodynamics.

Let us now proceed to a simple model of a ferromagnet FM sandwiched between two reservoirs NM with a temperature difference applied (Fig. 4b). When FM is sufficiently smaller than the magnetic domain wall width, all spins move in unison and the ferromagnet is characterized by a single macrospin temperature that determines the uniform fluctuations of the magnetization around the equilibrium direction.

We now have to consider the other degrees of freedom of the system — the phonons and, in conductors, the electrons. Electrons and phonons are relatively strongly coupled among themselves, but much less to the spins. We assume that electrons/phonons are thermalized, meaning that their distribution function can be represented by a temperature profile that interpolates between the hot and cold terminals, as indicated in Fig. 4, disregarding the thermal resistance of the interfaces. Because on the left side the magnet is now colder than the contact, the pumped spin current governed by the fluctuations corresponding to T_F is smaller than the spin current induced by the Johnson–Nyquist noise, which scales with electron temperature T_L. On the right-hand side the situation is the opposite. When the contacts are identical and in the steady state, the total spin (and heat currents) entering from the left and leaving on the right have to be the same, so $T_F = (T_L + T_R)/2$. We may conclude that a spin and heat current can be transported by the fluctuations of the magnetization. This mechanism works for either conducting or insulating ferromagnets.

The (transverse) spin Seebeck effect can now be explained by considering the situation for a Pt contact on top of a ferromagnet subject to a temperature bias. Even in Pt the spin–orbit interaction is considered a weak perturbation, so the ISHE generates a voltage for a spin current that may be computed as if injected into a simple metal. If the underlying ferromagnet is macroscopically large, a macrospin approximation is not appropriate. Instead of a single magnetic temperature T_F we have to consider now a magnon temperature distribution $T_F(x)$ which, as argued above, can differ from that of the electron–phonon system. The latter is assumed to be identical to T_N, the electron temperature in the normal metal, by effective thermalization. In the transverse configuration (Fig. 3e), the temperature difference $T_F - T_N$, and therefore the spin current and the associated ISHE signal, has to change sign between the hot and cold edges, as observed. Scattering theory leads to a predicted magnitude of the spin current in the transverse configuration of [76]

$$I_s(x) = \frac{\hbar\gamma}{2\pi}\frac{g_r}{M_s V_{coh}} k_B (T_F - T_N)(x) \qquad (4)$$

where γ is the gyromagnetic ratio, M_s the saturation magnetization, V_{coh} a magnetic coherence volume and k_B the Boltzmann constant. Adachi *et al.* subsequently arrived at a similar expression by linear response theory[77]. Equation (4) summarizes our qualitative understanding of the spin Seebeck effect but raises a few issues that have not all been resolved.

In the macrospin model the spin current is inversely proportional to the total magnetization volume, because the spin-torque pumping is a surface effect on the total magnetization. Without corrections this would lead to a very small signal in large samples. This issue can be resolved by the Landau–Lifshitz–Gilbert equation[78]: only those spins contribute that are close to interfaces within a magnetic coherence volume V_{coh}, which is a material parameter of the order of (10 nm)^3, scaling as $\sqrt{(T_F D^3)}$ where D is the spin-wave stiffness[76].

The magnitude of the mixing conductance is well established for intermetallic interfaces[79], but not for interfaces including magnetic insulators such as YIG. Although initial modelling with a simple Stoner model predicted a small mixing conductance that agreed with experiments, a local moment picture[50] and band structure calculations[80] found much larger values, comparable to those of intermetallic junctions. Recent dedicated experiments[81] indicate that by careful interface preparation the mixing conductance can be greatly increased to agree with theory.

Computing the spatial distribution of the non-equilibrium between electrons or phonons and magnetization is a difficult problem. In the simplest approximation the electrons or phonons, as well as elementary excitations of the magnet (the spin waves or magnons), are fully thermalized on a local scale. The problem then reduces to a simple diffusion picture of weakly coupled subsystems with proper boundary conditions[82], which seems to work well for YIG at room temperature[76]. This picture breaks down at low temperatures at which the phonon-drag effect on the magnons kicks in[83], explaining the strong enhancement of the spin Seebeck signal found in that regime for GaMnAs[84].

In ferromagnetic metals the mean free path length of the magnons is too small to explain the length scale observed in the spin Seebeck effect in the lateral configuration[64]. Coherent phonons in sample and substrate are therefore likely to be essential for the very observability of the effect in these materials. An important hint

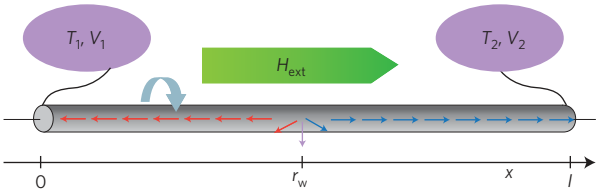

Figure 5 | Multifunctional magnetic nanomachine, consisting of a magnetic nanowire of length l, containing a domain wall centred at position r_w. The wire is in electrical and thermal contact with reservoirs that allow application of a temperature or voltage bias. The wire is mounted such that it can rotate around the *x* axis. A magnetic field and mechanical torque can be applied along *x*. Figure reprinted with permission from ref. 54, © 2010 APS.

was the observation that the spin Seebeck effect is robust against 'scratches' in the ferromagnetic film, proving that the substrate plays an important role[84]. Further evidence comes from the amplitude of the spin-Seebeck effect in GaMnAs, which was found to scale with the thermal conductivity of the GaAs substrate and the phonon-drag contribution to the thermoelectric power of the GaMnAs, demonstrating that phonons drive the spin redistribution[84]. The presence of the coupling of magnons to coherent phonons in sample and substrate explains the spin Seebeck effect even for a single magnetic wire rather than an extended film[85]. This phenomenon is clearly beyond the drift-diffusion model for the magnon–phonon system, and can be explained for YIG by the linear response formalism[77,83]. Some progress has been made in understanding how the interaction between magnons and conduction-electron spins affects the spin-dependent Seebeck effect[42], and in understanding the magnon contribution to the dissipative spin-transfer torque parameter β_c (ref. 43), but a microscopic theory for the spin Seebeck effect in ferromagnetic metals is still lacking.

Initially, experiments were carried out in the 'transverse configuration' of Fig. 3e. However, the 'longitudinal configuration' in Fig. 3d is the most basic set-up for the study and application of the spin Seebeck effect in insulators[86,87]. For the former configuration, precise temperature-distribution control and careful choice of substrates are important[71]. Otherwise, signals may be contaminated by artefacts such as the anomalous Nernst[88] effect (see below). An experiment on ferromagnetic metals would in principle display both the spin Seebeck and spin-dependent Seebeck effect observed by Slachter *et al.*[22], but detection by the ISHE is very difficult. Weiler *et al.*[89] carried out a spatially resolved study on Pt|F bilayers for conducting and insulating ferromagnets. Whereas for Pt|YIG the longitudinal spin Seebeck effect was detected, the Hall voltages of Pt|Co_2FeAl turned out to be dominated by the anomalous Nernst effect[76,78] (see below).

The longitudinal spin Seebeck effect in cooperation with the ISHE converts heat flows into electric voltages that increase linearly with size and do not require complicated thermopile structuring. Therefore, it could be used as a large-area electric power generator driven by heat (A. Kirihara *et al.*, manuscript in preparation). The standard thermoelectric figure of merit must be reconsidered, as the heat conductivity is no longer a relevant parameter, opening the way to new strategies to increase the efficiency of thermopower generation. Applications of the spin Seebeck effect in the longitudinal configuration to position-sensitive detectors have been proposed[90]. In the longitudinal configuration the spin pumping can be driven by ultrasound excitation as well[85].

As mentioned above, the physics of the thermal torque induced by heat currents in spin valves with an insulator as polarizing magnet as proposed by Slonczewski[50] is identical to that of the longitudinal spin Seebeck effect. The 'loose' magnetic monolayer model hypothesized by Slonczewski seems to mimic the coherence volume V_{coh} that follows from the Landau–Lifshitz–Gilbert equation.

The interaction between charge currents and magnetization dynamics can be cast into a linear response matrix that obeys Onsager reciprocity relations[38], which can be extended to include heat currents and temperature differences. Therefore, the spin Peltier effect — the cooling of the magnetization of a ferromagnetic insulator by a proximity spin accumulation — must exist as the Onsager equivalent of the spin Seebeck effect.

Spin caloritronic heat engines and motors. Onsager's reciprocal relations[13] reveal that seemingly unrelated phenomena can be expressions of identical microscopic correlations between thermodynamic variables of a given system[14]. The archetypal example is the Onsager–Kelvin identity of thermopower and Peltier cooling (Box 1). The Onsager equivalency between particle-current-induced spin-transfer torque and spin pumping, on the other hand, is a recent insight[38]. The reciprocity of heat-current-induced spin transfer torque and spin pumping by thermal fluctuations follows from an analogous treatment by scattering theory. The results in linear response for a magnetic wire incorporating a tail-to-tail magnetic domain wall (Fig. 5) lead to the proposal of spin caloritronic heat engines[53,54,63,91]. Mechanical and magnetic motions are coupled by the Barnett and Einstein–de Haas effects[92–94], which are again each other's Onsager reciprocals[54]. The thermoelectric response matrix including all these variables can be formulated for a simple model system consisting of a rotatable magnetic wire including a rigid domain wall parameterized by its width and position r_w (see Fig. 5). The mechanical torque induced by temperature differences may be interpreted in terms of Feynman's ratchet and pawl in the continuum limit. The pawl providing mechanical chirality in the latter is replaced in the former by the magnetic order.

Such a machine has multiple functionalities: it can be operated as an electric generator and dynamo (for metallic ferromagnets only), a thermally driven Brownian motor or a mechanically driven cooler (also for insulating magnets).

Relativistic effects

Thermal Hall effects exist in normal metals in the presence of external magnetic fields and can be classified into three groups[95]. The Nernst effect represents the Hall voltage induced by a heat current. The Nettingshausen effect describes the heat current that

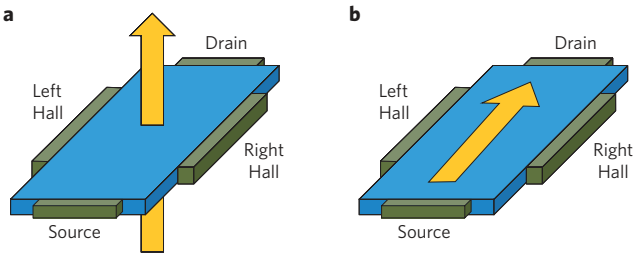

Figure 6 | Hall effects in ferromagnets. A sketch of the configuration for **a**, anomalous Hall effects and **b**, planar Hall effects. Source, drain, left and right Hall contacts connect to reservoirs at controlled temperature and electrochemical potentials. The arrow denotes whether the magnetization direction is normal to or in the film plane. The signal modulation as a function of in-plane angle is also referred to as anisotropic. A typical thermoelectric experiment consists of measuring the transverse Hall voltage difference induced by a source–drain temperature bias, the anomalous Nernst effect in configuration **a** or planar or anisotropic Nernst effect in configuration **b**. Note that the effects in the absence of magnetization receive the label 'spin', such as the inverse spin Hall effect in Fig. 4c, referring to the Hall voltage induced by a source–drain spin current.

is induced transverse to an applied charge current. The Hall heat current induced by a temperature gradient goes by the name of the Righi–Leduc effect. The spin degree of freedom opens a family of spin caloritronic Hall effects in the absence of an external field, and these are not yet fully explored. We may add the label 'spin' in order to describe effects in normal metals (spin Hall effect, spin Nernst effect and so on). In ferromagnets we may distinguish the configuration in which the magnetization is normal to both currents (anomalous Hall effect, anomalous Nernst effect and so forth) from the configuration with in-plane magnetization (planar Hall effect, anisotropic magnetoresistance, planar Nernst effect and so on) as sketched in Fig. 6. Theoretical work has been carried out with emphasis on the intrinsic spin–orbit interaction[96–98]. The thermoelectric figure of merit could possibly be improved by making use of the conducting edge and surface states of topological insulators[99].

Seki *et al.*[100,101] found experimental evidence for a thermal Hall effect in Au/FePt structures, which could be due either to an anomalous Nernst effect in FePt or to a spin Nernst effect in Au. In GaMnAs, planar[102] and anomalous[103] Nernst effects have been observed, with intriguing temperature dependences. Slachter *et al.*[104] identified the anomalous Nernst effect and an anisotropic magnetoheating effect in a multiterminal permalloy/Cu spin valve. The anomalous Nernst effect is rather ubiquitous and may interfere with other spin caloritronics effects[71,84,88,89].

The heat is on

Spin caloritronics has gained momentum in recent years with the entry of several new groups and even research consortia into the field. Much has yet to be done. Many effects predicted by theory have not yet been observed, and unexpected phenomena such as the spin Seebeck effect might still wait for their discovery. If spin caloritronics is to become more than a scientific curiosity, the thermoelectric figures of merit should be increased. The tunnel (magneto) Seebeck effect is already fairly large, and carries the promise of useful applications, as does the extreme simplicity of spin Seebeck devices. More materials research and device engineering, experimental and theoretical, however, is clearly needed.

References

1. Ashcroft, N. W. & Mermin, N. D. *Solid State Physics* (Saunders, 1976).
2. Nolas, G. S., Sharp, J. & Goldsmid, H. J. *Thermoelectrics: Basic Principles and New Materials Developments* (Springer, 2001).
3. Johnson, M. & Silsbee, R. H. Thermodynamic analysis of interfacial transport and of the thermomagnetoelectric system. *Phys. Rev. B* **35,** 4959–4972 (1987).
4. Shi, J. *et al.* Field-dependent thermoelectric power and thermal conductivity in multilayered and granular giant magnetoresistive systems. *Phys. Rev. B* **54,** 15273–15283 (1996).
5. Gravier, L., Guisan, S. S., Reuse, F. & Ansermet, J-Ph. Spin-dependent Peltier effect of perpendicular currents in multilayered nanowires. *Phys. Rev. B* **73,** 052410 (2006).
6. Bauer, G. E. W., MacDonald, A. H. & Maekawa, S. Spin caloritronics. *Solid State Commun.* **150,** 459–460 (2010).
7. Giazotto, F., Heikkilä, T. T., Luukanen, A., Savin, A. M. and Pekola, J. P. Opportunities for mesoscopics in thermometry and refrigeration: physics and applications. *Rev. Mod. Phys.* **78,** 217–274 (2006).
8. Dubi, Y. & Di Ventra, M. Colloquium: Heat flow and thermoelectricity in atomic and molecular junctions. *Rev. Mod. Phys.* **83,** 131–155 (2011).
9. Wong, C. H., van Driel, H. J., Kittinaradorn, R., Stoof, H. T. C. & Duine, R. A. Spin caloritronics in noncondensed Bose gases. *Phys. Rev. Lett.* **108,** 075301 (2012).
10. Hatami, M., Bauer, G. E. W., Zhang, Q. & Kelly, P. J. Thermal spin-transfer torque in magnetoelectronic devices. *Phys. Rev. Lett.* **99,** 066603 (2007).
11. Hatami, M., Bauer, G. E. W., Zhang, Q. & Kelly, P. J. Thermoelectric effects in magnetic nanostructures. *Phys. Rev. B* **79,** 174426 (2009).
12. Takezoe, Y., Hosono, K., Takeuchi, A. & Tatara, G. Theory of spin transport induced by a temperature gradient. *Phys. Rev. B* **82,** 094451 (2010).
13. Onsager, L. Reciprocal relations in irreversible processes, I. *Phys. Rev.* **37,** 405–426 (1931).
14. De Groot, S. R. *Thermodynamics of Irreversible Processes* (Interscience, 1952).
15. Heikkilä, T. T., Hatami, M. & Bauer, G. E. W. Spin heat accumulation and its relaxation in spin valves. *Phys. Rev. B* **81,** 100408 (2010).
16. Heikkilä, T. T., Hatami, M. & Bauer, G. E. W. Electron–electron interaction induced spin thermalization in quasi-low-dimensional spin valves. *Solid State Commun.* **150,** 475–479 (2010).
17. Serrano-Guisan, S. *et al.* Enhanced magnetic field sensitivity of spin-dependent transport in cluster-assembled metallic nanostructures. *Nature Mater.* **5,** 730–734 (2006).
18. Tsyplyatyev, O., Kashuba, O. & Fal'ko, V. I. Thermally excited spin current and giant magnetothermopower in metals with embedded ferromagnetic nanoclusters. *Phys. Rev. B* **74,** 132403 (2006).
19. Scharf, B., Matos-Abiague, A. ,Žutić, I. & Fabian, J. Theory of thermal spin-charge coupling in electronic systems. *Phys. Rev. B* **85,** 085208 (2012).
20. Sugihara, A. *et al.* Giant Peltier effect in a submicron-sized Cu–Ni/Au junction with nanometer-scale phase separation. *Appl. Phys. Express* **3,** 065204 (2010).
21. Vu, N. D., Sato, K. & Katayama-Yoshida, H. Giant Peltier effect in self-organized quasi-one-dimensional nano-structure in Cu–Ni alloy. *Appl. Phys. Express* **4,** 015203 (2011).
22. Slachter, A., Bakker, F. L., Adam, J. P. & van Wees, B. J. Thermally driven spin injection from a ferromagnet into a non-magnetic metal. *Nature Phys.* **6,** 879–882 (2010).
23. Flipse, J., Bakker, F. L., Slachter, A., Dejene, F. K. & van Wees, B. J. Direct observation of the spin-dependent Peltier effect. *Nature Nanotech.* **7,** 166–168 (2012).
24. Gönnenwein, S. & Bauer, G. E. W. Electron spins blow hot and cold. *Nature Nanotech.* **7,** 145–147 (2012).
25. Wang, Z. C., Su, G. & Gao, S. Spin-dependent thermal and electrical transport in spin-valve system. *Phys. Rev. B* **63,** 224419 (2000).
26. McCann, E. & Fal'co, V. I. Giant magnetothermopower of magnon-assisted transport in ferromagnetic tunnel junctions. *Phys. Rev. B* **66,** 134424 (2002).
27. Liebing, N. *et al.* Tunneling magnetothermopower in magnetic tunnel junction nanopillars. *Phys. Rev. Lett.* **107,** 177201 (2011).
28. Walter, M. *et al.* Seebeck effect in magnetic tunnel junctions. *Nature Mater.* **10,** 742–746 (2011).
29. Czerner, M., Bachmann, M. & Heiliger, C. Spin caloritronics in magnetic tunnel junctions: ab initio studies. *Phys. Rev. B* **83,** 132405 (2011).
30. Jia, X., Liu, K., Xia, K. & Bauer, G. E. W. Thermal spin transfer in Fe–MgO–Fe tunnel junctions. *Phys. Rev. Lett.* **107,** 176603 (2011).
31. Lin, W. *et al.* Giant thermoelectric effect in Al_2O_3 magnetic tunnel junctions. *Nature Commun.* **3,** 744 (2012).
32. Maslyuk, V. V. Achilles, S. & Mertig, I. Spin-polarized transport and thermopower of organometallic nanocontacts. *Solid State Commun.* **150,** 505–509 (2010).
33. Jansen, R. Silicon spintronics. *Nature Mater.* **11,** 400–408 (2012).
34. Le Breton, J-C., Sharma, S., Saito, H., Yuasa, S. & Jansen, R. Thermal spin current from a ferromagnet to silicon by Seebeck spin tunneling. *Nature* **475,** 82–85 (2011).
35. Naydenova, Ts. *et al.* Diffusion thermopower of (Ga, Mn)As/GaAs tunnel junctions. *Phys. Rev. Lett.* **107,** 197201 (2011).
36. Kruglyak, V. V., Demokritov, S. O. & Grundler, D. Magnonics. *J. Phys. D: Appl. Phys.* **43,** 26030 (2010).
37. Lenk, B., Ulrichs, H., Garbs, F. & Münzenberg, M. The building blocks of magnonics. *Phys. Rep.* **507,** 107–136 (2011).
38. Brataas, A., Kent, A. D. & Ohno, H. Current-induced torques in magnetic materials. *Nature Mater.* **11,** 372–381 (2012).
39. Hess, C. Heat conduction in low-dimensional quantum magnets. *Eur. Phys. J. Spec. Topics* **151,** 73–83 (2007).
40. Meier, F. & Loss, D. Magnetization transport and quantized spin conductance. *Phys. Rev. Lett.* **90,** 167204 (2003).
41. Vlaminck, V. & Bailleul, M. Current-induced spin-wave Doppler shift. *Science* **322,** 410–413 (2008).
42. Tulapurkar, A. A. & Suzuki, Y. Contribution of electron–magnon scattering to the spin-dependent Seebeck effect in a ferromagnet. *Solid State Commun.* **150,** 466–470 (2010).
43. Lucassen, M. E., Wong, C. H., Duine, R. A. & Tserkovnyak, Y. Spin-transfer mechanism for magnon-drag thermopower. *Phys. Rev. Lett.* **99,** 262506 (2011).
44. Costache, M. V., Bridoux, G., Neumann, I. & Valenzuela, S. O. Magnon-drag thermopile. *Nature Mater.* **11,** 199–202 (2012).
45. Kajiwara, Y. *et al.* Transmission of electrical signals by spin-wave interconversion in a magnetic insulator. *Nature* **464,** 262–266 (2010).
46. Beaurepaire, E., Merle, J-C., Daunois, A. & Bigot, J-Y. Ultrafast spin dynamics in ferromagnetic nickel. *Phys. Rev. Lett.* **76,** 4250–4253 (1996).
47. Ralph, D. C. & Stiles, M. D. *J. Magn. Magn. Mater.* **320,** 1190–1216 (2008).
48. Wegrowe, J. E. Spin transfer from the point of view of the ferromagnetic degrees of freedom. *Solid State Commun.* **150,** 519–523 (2010).

49. Yu, H., Granville, S., Yu, D. P. & Ansermet, J-Ph. Evidence for thermal spin-transfer torque. *Phys. Rev. Lett.* **104,** 146601 (2010).
50. Slonczewski, J. C. Initiation of spin-transfer torque by thermal transport from magnons. *Phys. Rev. B* **82,** 054403 (2010).
51. Zhang, S. & Li, Z. Roles of nonequilibrium conduction electrons on the magnetization dynamics of ferromagnets. *Phys. Rev. Lett.* **93,** 127204 (2004).
52. Tserkovnyak, Y., Brataas, A. & Bauer, G. E. W. Theory of current-driven magnetization dynamics in inhomogeneous ferromagnets. *J. Magn. Magn. Mater.* **320,** 1282–1292 (2008).
53. Kovalev, A. A. & Tserkovnyak, Y. Thermoelectric spin transfer in textured magnets. *Phys. Rev. B* **80,** 100408 (2009).
54. Bauer, G. E. W., Bretzel, S., Brataas, A. & Tserkovnyak, Y. Nanoscale magnetic heat pumps and engines. *Phys. Rev. B* **81,** 024427 (2010).
55. Hals, K. M. D., Brataas, A. & Bauer, G. E. W. Thermopower and thermally induced domain wall motion in (Ga, Mn)As. *Solid State Commun.* **150,** 461–465 (2010).
56. Yuan, Z., Wang, S. & Xia, K. Thermal spin-transfer torques on magnetic domain walls. *Solid State Commun.* **150,** 548–551 (2010).
57. Möhrke, P., Rhensius, J., Thiele, J-U., Heyderman, L. J. & Kläui, M. Tailoring laser-induced domain wall pinning. *Solid State Commun.* **150,** 489–491 (2010).
58. Mikhallov, A. V. & Yaremchuk, A. I. Forced motion of a domain wall in the field of a spin wave. *JETP Lett.* **39,** 354–357 (1984).
59. Yaremchuk, A. I. Interaction of domain wall with a spin wave in the framework of an integrable case of the Landau–Lifshitz equations. *Teoret. Mat. Fiz.* **62,** 153–158 (1985).
60. Han, D-S. *et al.* Magnetic domain-wall motion by propagating spin waves. *Appl. Phys. Lett.* **94,** 112502 (2009).
61. Hinzke, D. & Nowak, U. Domain wall motion by the magnonic spin Seebeck effect. *Phys. Rev. Lett.* **107,** 027205 (2011).
62. Yan, P., Wang, X. S. & Wang, X. R. All-magnonic spin-transfer torque and domain wall propagation. *Phys. Rev. Lett.* **107,** 177207 (2011).
63. Kovalev, A. A. & Tserkovnyak, Y. Thermomagnonic spin transfer in textured magnets. *Europhys. Lett.* **97,** 67002 (2012).
64. Uchida, K. *et al.* Spin-Seebeck effects in NiFe/Pt films. *Solid State Commun.* **150,** 524–528 (2010).
65. Saitoh, E., Ueda, M., Miyajima, H. & Tatara, G. Conversion of spin current into charge current at room temperature: inverse spin-Hall effect. *Appl. Phys. Lett.* **88,** 182509 (2006).
66. Valenzuela, S. O. & Tinkham, M. Direct electronic measurement of the spin Hall effect. *Nature* **442,** 176–179 (2006).
67. Kimura, T., Otani, Y., Sato, T. Takahashi, S. & Maekawa, S. Room-temperature reversible spin Hall effect. *Phys. Rev. Lett.* **98,** 156601 (2007).
68. Jungwirth, T., Wunderlich, J. & Olejnik, K. Spin Hall effect devices. *Nature Mater.* **11,** 382–390 (2012).
69. Uchida, K. *et al.* Spin Seebeck insulator. *Nature Mater.* **9,** 894–897 (2010).
70. Jaworski, C. M. *et al.* Observation of the spin-Seebeck effect in a ferromagnetic semiconductor. *Nature Mater.* **9,** 898–903 (2010).
71. Bosu, S. *et al.* Spin Seebeck effect in thin films of the Heusler compound Co_2MnSi. *Phys. Rev. B* **83,** 224401 (2011).
72. Hatami, M., Bauer, G. E. W., Takahashi, S. & Maekawa, S. Thermoelectric spin diffusion in a ferromagnetic metal. *Solid State Commun.* **150,** 480–484 (2010).
73. Nunner, T. S. & von Oppen, F. Quasilinear spin-voltage profiles in spin thermoelectrics. *Phys. Rev. B* **84,** 020405 (2011).
74. Tserkovnyak, Y., Brataas, A., Bauer, G. E. W. & Halperin, B. I. Nonlocal magnetization dynamics in ferromagnetic heterostructures. *Rev. Mod. Phys.* **77,** 1375–1421 (2005).
75. Foros, J., Brataas, A., Tserkovnyak, Y. & Bauer, G. E. W. Magnetization noise in magnetoelectronic nanostructures. *Phys. Rev. Lett.* **95,** 016601 (2005).
76. Xiao, J., Bauer, G. E. W., Uchida, K., Saitoh, E. & Maekawa, S. Theory of magnon-driven spin Seebeck effect. *Phys. Rev. B* **81,** 214418 (2010).
77. Adachi, H., Ohe, J., Takahashi, S. & Maekawa, S. Linear-response theory of spin Seebeck effect in ferromagnetic insulators. *Phys. Rev. B* **83,** 094410 (2011)
78. Ohe, J., Adachi, H., Takahashi, S. & Maekawa, S. Numerical study on the spin Seebeck effect. *Phys. Rev. B* **83,** 115118 (2011).
79. Brataas, A., Bauer, G. E. W. & Kelly, P. J. Non-collinear magnetoelectronics. *Phys. Rep.* **427,** 157–255 (2006).
80. Jia, X., Liu, K., Xia, K. & Bauer, G. E. W. Spin transfer torque on magnetic insulators. *Europhys. Lett.* **96,** 17005 (2011).
81. Burrowes, C. B. *et al.* Enhanced spin pumping at yttrium iron garnet/Au interfaces. *Appl. Phys. Lett.* **100,** 092403 (2012).
82. Sanders, D. J. & Walton, D. Effect of magnon-phonon thermal relaxation on heat transport by magnons. *Phys. Rev. B* **15,** 1489–1494 (1977).
83. Adachi, H. *et al.* Gigantic enhancement of spin Seebeck effect by phonon drag. *Appl. Phys. Lett.* **97,** 252506 (2010).
84. Jaworski, C. M. *et al.* Spin-Seebeck effect: a phonon driven spin distribution. *Phys. Rev. Lett.* **106,** 186601 (2011).
85. Uchida, K. *et al.* Long-range spin Seebeck effect and acoustic spin pumping. *Nature Mater.* **10,** 737–741 (2011).
86. Uchida, K., Nonaka, T, Ota, T. & Saitoh, E. Observation of longitudinal spin-Seebeck effect in magnetic insulators. *Appl. Phys. Lett.* **97,** 172505 (2010).
87. Uchida, K. *et al.* Thermal spin pumping and magnon-phonon-mediated spin-Seebeck effect. Preprint at http://arxiv.org/abs/1111.3036 (2011).
88. Huang, S. Y., Wang, W. G., Lee, S. F., Kwo, J. & Chien, C. L. Intrinsic spin-dependent thermal transport. *Phys. Rev. Lett.* **107,** 216604 (2011).
89. Weiler, M. *et al.* Local charge and spin currents in magnetothermal landscapes. *Phys. Rev. Lett.* **108,** 106602 (2012).
90. Uchida, K., Kirihara, A., Ishida, M., Takahashi, R. & Saitoh, E. Local spin-Seebeck effect enabling two-dimensional position sensing. *Jpn. J. Appl. Phys.* **50,** 120211 (2011).
91. Kovalev, A. A. & Tserkovnyak ,Y. Magnetocaloritronic nanomachines. *Solid State Commun.* **150,** 500–504 (2010).
92. Barnett, S. J. Magnetization by rotation. *Phys. Rev.* **6,** 239–270 (1915).
93. Barnett, S. J. Gyromagnetic and electron-inertia effects. *Rev. Mod. Phys.* **7,** 129–167 (1935).
94. Einstein A. & de Haas, W. J. Experimental proof of Ampère's molecular currents. *Deutsche Phys. Ges. Verh.* **17,** 152–170 (1915).
95. Callen, H. B. The application of Onsager's reciprocal relations to thermoelectric, thermomagnetic, and galvanomagnetic effects. *Phys. Rev.* **73,** 1349–1358 (1948).
96. Onoda, S. Sugimoto, N. & Nagaosa, N. Quantum transport theory of anomalous electric, thermoelectric, and thermal Hall effects in ferromagnets. *Phys. Rev. B* **77,** 165103 (2008).
97. Ma, Z. Spin Hall effect generated by a temperature gradient and heat current in a two-dimensional electron gas. *Solid State Commun.* **150,** 510–513 (2010).
98. Liu X. & Xie, X. C. Spin Nernst effect in the absence of a magnetic field. *Solid State Commun.* **150,** 471–474 (2010).
99. Tretiakov, O. A., Abanov, A., Murakami, S. & Sinova, J. Large thermoelectric figure of merit for 3D topological Anderson insulators via line dislocation engineering. *Appl. Phys. Lett.* **97,** 073108 (2010).
100. Seki, T. *et al.* Giant spin Hall effect in perpendicularly spin-polarized FePt/Au devices. *Nature Mater.* **7,** 125–129 (2008).
101. Seki, T., Sugai, I., Hasegawa, Y., Mitani, S. & Takanashi, K. Spin Hall effect and Nernst effect in FePt/Au multi-terminal devices with different Au thicknesses. *Solid State Commun.* **150,** 496–499 (2010).
102. Pu, Y., Johnston-Halperin, E., Awschalom, D. D. & Shi, J. Anisotropic thermopower and planar Nernst effect in $Ga_{1-x}Mn_xAs$ ferromagnetic semiconductors. *Phys. Rev. Lett.* **97,** 036601 (2006).
103. Pu, Y., Chiba, D., Matsukura, F., Ohno, H. & Shi, J. Mott relation for anomalous Hall and Nernst effects in $Ga_{1-x}Mn_xAs$ ferromagnetic semiconductors. *Phys. Rev. Lett.* **101,** 117208 (2008).
104. Slachter, A., Bakker, F. L. & van Wees, B. J. Modeling of thermal spin transport and spin–orbit effects in ferromagnetic/nonmagnetic mesoscopic devices. *Phys. Rev. B* **84,** 020412 (2011).
105. Butcher, P. N. Thermal and electrical transport formalism for electronic microstructures with many terminals. *J. Phys. Condens. Matter* **2,** 4869–4878 (1990).

Acknowledgements

We are grateful for collaboration with F. Bakker, A. Brataas, X. Jia, M. Hatami, T. Heikillä, P. Kelly, S. Maekawa, B. Slachter, S. Takahashi, K. Takanashi, Y. Tserkovnyak, K. Uchida, K. Xia, J. Xiao and many others. This work was supported in part by the FOM Foundation, EU-ICT-7 'MACALO', and DFG Priority Programme 1538 'Spin-Caloric Transport'.

Additional information

The authors declare no competing financial interests. Reprints and permissions information is available online at http://npg.nature.com/reprintsandpermissions. Correspondence should be addressed to G.E.W.B.